ACS APPLIED MATERIALS & INTERFACES
Research Article
www.acsami.org

Enhancing the Performance of Polymer Photovoltaic Cells by Using an Alcohol Soluble Fullerene Derivative as the Interfacial Layer

Qiang Mei,[†] Cuihong Li,*,[†] Xue Gong,[†] Heng Lu,[†] Enquan Jin,[†] Chun Du,[†] Zhen Lu,[†] Li Jiang,[‡] Xiangyue Meng,[‡] Chunru Wang,[‡] and Zhishan Bo*,[†]

[†] Beijing Key Laboratory of Energy Conversion and Storage Materials, College of Chemistry, Key Laboratory of Theoretical and Computational Photochemistry, Ministry of Education, Beijing Normal University, Beijing 100875, China

[‡] Institute of Chemistry, Chinese Academy of Sciences, Beijing 100190, China

Supporting Information

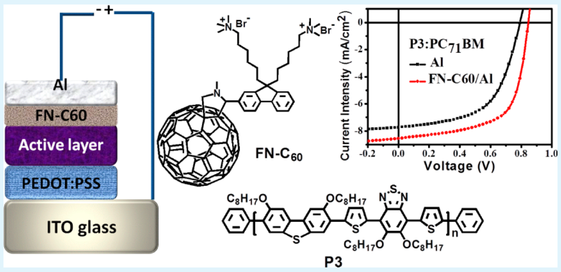

ABSTRACT: Alcohol soluble fullerene derivative (**FN-C60**) has been synthesized and used as a cathode interfacial layer for high-efficiency polymer solar cells (PSCs). To examine the function of the **FN-C60** interfacial layer, polymer solar cells were fabricated with blends of **P3**:$PC_{71}BM$, **HXS-1**:$PC_{71}BM$, **PDFCDTBT**:$PC_{71}BM$, and **PDPQTBT**:$PC_{71}BM$ as the active layer. In comparison to the bare Al electrode, power conversion efficiencies (PCEs) of **P3**:$PC_{71}BM$, **HXS-1**:$PC_{71}BM$, **PDFCDTBT**:$PC_{71}BM$, and **PDPQTBT**:$PC_{71}BM$ based PSCs were increased from 3.50 to 4.64%, 4.69 to 5.25%, 2.70 to 4.60%, and 1.52 to 2.29%, respectively, when **FN-C60**/Al was used as the electrode. Moreover, the overall photovoltaic performances of PSCs with the **FN-C60**/Al electrode were better than those of cells with LiF/Al electrode, indicating that **FN-C60** is a potential interfacial layer material to replace LiF.

KEYWORDS: *fullerene derivative, alcohol soluble, interfacial layer, photovoltaic performance, polymer solar cells, power conversion efficiency*

INTRODUCTION

Due to their obvious advantages such as low weight, low cost, and easy production via roll-to-roll processing, polymer solar cells (PSCs) have attracted tremendous attend both from the scientic community and industry.[1−15] The performance of polymer solar cells has experienced a rapid development over the past few years, and the power conversion efficiency (PCE) has reached 9% for single junction solar cells[16] and 12% for tandem solar cells.[17]

For single junction polymer solar cells, two different device structures, namely conventional structure and inverted structure, are commonly used. The conventional polymer solar cell device structure is composed of glass/indium tin oxide (ITO)/poly(3,4-ethylenedioxythiophene) (PEDOT):poly(styrenesulfonate) (PSS)/active layer/interfacial layer/Al; the active layer is a blend of donor and acceptor; and usually, a thin layer of calcium with a thickness of about 10 nm was used as the interfacial layer between the active layer and aluminum cathode. Al is commonly used as the electron collecting electrode in bulk heterojunction polymer solar cell (BHJ PSC) devices. To achieve highly efficient PSCs, it is critical to improve the electron collection of the Al electrode and suppress the hole collection. The interfacial layer plays a pivotal role in determining the PCE of PSCs. First, the interfacial layer can tune the energy level alignment at the electrode/active layer interface.[18−21] The use of an appropriate interlayer can decrease the contact resistance between the active layer and the electrode to achieve Ohmic contact and thus maximize the open-circuit voltage (V_{oc}), since the maximum achievable V_{oc}, which is dependent on the difference between the quasi-Fermi levels of the photoinduced holes in the donor and the photoinduced electrons in the acceptor, can be realized only Ohmic contacts are formed with both cathode and anode.[22,23] Second, the interfacial layer can be used to tune the work functions of both bottom and top electrodes, and the use of appropriate interfacial layer can increase the charge extraction efficiency and selectivity.[24,25] To achieve these goals, many efforts have been devoted to modify the interface between Al and the organic active layer to alter the contact properties and improve the PCE of BHJ PSCs.[26,27] For example, the use of a thermally deposited thin film of LiF or Ca before Al deposition can improve electron collection ability, V_{oc}, short circuit current (J_{sc}), fill factor (FF), and, thus, the PCE over 20%.[20,22,28] However, the requirement of high vacuum for the deposition of LiF or the Ca layer is not compatible with the large scale solution processing technique, which is the most obvious advantage of polymer-based cells. Meanwhile, the photovoltaic performance is extremely sensitive to the thickness of the LiF layer, which must be very thin (0.3−0.5 nm).[28] Such thin thickness is difficult to be precisely controlled during vacuum

Received: June 4, 2013
Accepted: July 23, 2013
Published: July 23, 2013

ACS Publications © 2013 American Chemical Society

Scheme 1. Chemical Structure and Synthetic Route of FN-C60[a]

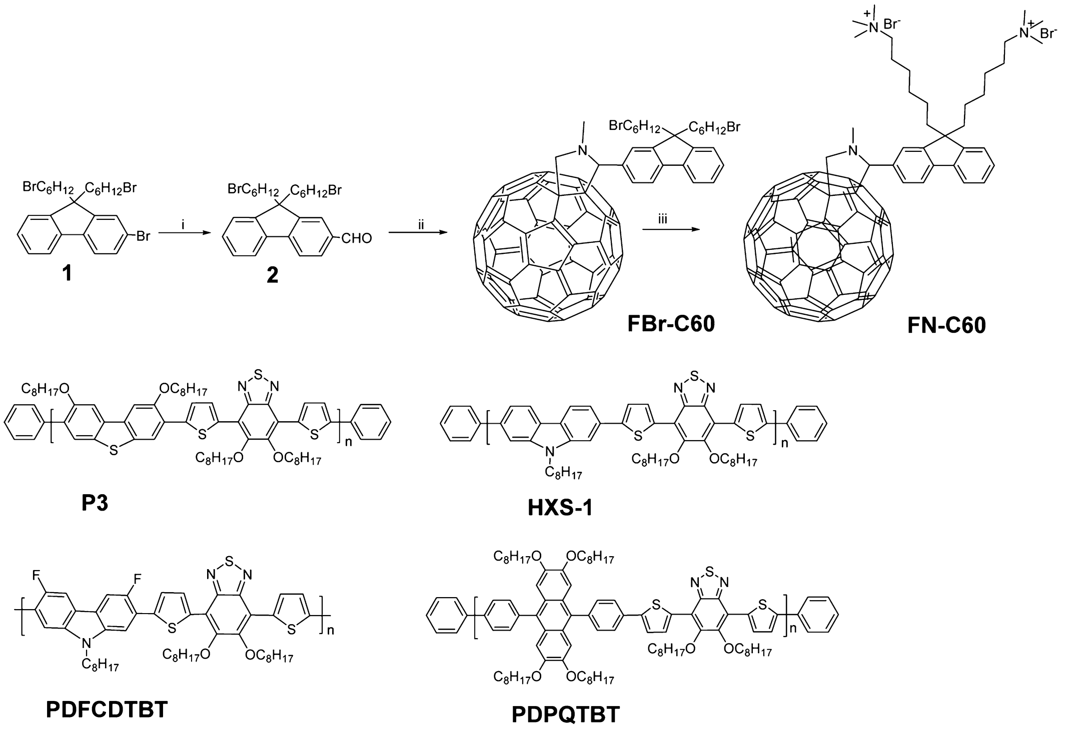

[a]Reagents and conditions: (i) *n*-BuLi, *N*,*N*-dimethylformamide (DMF); (ii) CH_3NHCH_2COOH, C_{60}, toluene, reflux, 2 h; (iii) $N(CH_3)_3$/alcohol, room temperature, 72 h.

deposition. For the Ca interfacial layer, it is extremely sensitive to moisture and air.[24,25] Additionally, self-assembled monolayers (SAMs)[29,30] and metal oxides (i.e., $CsCO_3$, TiO_x, MoO_3, and ZnO) have also been used as the interfacial layer in BHJ PSCs.[26,31−36] Recently, conjugated polyelectrolytes (CPEs) have been reported as the interfacial layer materials in BHJ PSCs to achieve increases in PCE.[37−40] Their solubility in highly polar solvents allows the simple fabrication of the interlayer without damaging the organic active layer that is typically miscible in aromatic solvents.

It is generally believed that the incorporation of an additional n-type C60 derivative interlayer between the electrode and the organic active layer as a hole blocking layer can improve the electron collection ability of the electrode to achieve enhanced device performance.[41,42] Jen and co-workers have reported that the incorporation of a self-assembled monolayer (SAM) of C60 derivative with a carboxylic acid group on the metal oxide surface can improve the performance of the inverted polymer solar cells.[29] Bäuerle et al. reported that a thermal evaporated 15 nm thick C60 interfacial layer between ITO and the organic active layer can be a very efficient device structure for organic solar cells.[43] Hsu and co-workers have reported the cross-linked fullerene derivative C-PCBSD (PCBSD) can be used as an effective electron transporting layer (ETL) and interfacial layer on top of ZnO or TiO_x in inverted solar cells, which have achieved superior device performance and remarkable long-term stability.[44,45] Very recently, Jen et al. reported the fabrication of an interfacial layer for the cathode using solution processed alcohol soluble fullerene surfactants.[46,47]

In this contribution, we have developed a new alcohol soluble fullerene derivative (**FN-C60**) as the interfacial material for cathode. The **FN-C60** interfacial layer was fabricated by spin-coating from an alcoholic solution without damaging the already spin-coated organic active layer. To examine the properties of the **FN-C60** interfacial layer, four different active layers, **P3**:$PC_{71}BM$, **HXS-1**:$PC_{71}BM$, **PDFCDTBT**:$PC_{71}BM$, and **PDPQTBT**:$PC_{71}BM$ were tested in this study. The chemical structures of **P3**, **HXS-1**, **PDFCDTBT**, and **PDPQTBT** are shown in Scheme 1. Conventional BHJ PSCs were fabricated. For **P3**:$PC_{71}BM$ based solar cells, the PCE was markedly enhanced from 3.50% for a bare Al electrode to 4.64% for a **FN-C60**/Al electrode. For **HXS-1**:$PC_{71}BM$ based solar cells, the PCE was improved from 4.69% for a bare Al electrode to 5.25% for a **FN-C60**/Al electrode. For **PDFCDTBT** and **PDPQTBT** based PSCs, PCEs were increased from 2.70 to 4.60% and 1.52 to 2.29%, respectively, when **FN-C60**/Al was used instead of bare Al as the electrode. The enhanced photovoltaic performance can be attributed to the simultaneous increase of V_{oc}, J_{sc}, and FF. Moreover, the overall photovoltaic characteristics of PSCs with the **FN-C60**/Al electrode were better than those with LiF/Al electrode, indicating that alcohol soluble fullerene derivative **FN-C60** is very promising as interfacial layer for BHJ PSCs.

■ RESULTS AND DISCUSSION

Material Synthesis and Characterization. The synthesis of **FN-C60** is outlined in Scheme 1. Starting from compound **1**,[48,49] its treatment with *n*-BuLi at −78 °C was followed by quenching with dimethyl formamide (DMF) to afford aldehyde **2** in a yield of 83%. The reaction of large excesses of C60 with aldehyde **2** and *N*-methylglycine by using 1,3-dipolar cycloaddition, namely, Prato reaction, was performed to afford **FBr-C60** in a yield of 11%.[50] The purification of **FBr-C60** was performed by column chromatography on a silica gel column and followed by preparative HPLC. The structure of **FBr-C60** was verified by ^1H NMR and matrix-assisted laser desorption ionization time-of-flight mass spectrometry (MALDI-TOF MS). The treatment of **FBr-C60** with $N(CH_3)_3$ in a solvent mixture of tetrahydrofuran (THF) and methanol at room temperature for 72 h afforded the aimed **FN-C60** in a yield of 79%. **FN-C60** can be dissolved in high polarity solvent, such as methanol, ethanol, DMF, dimethyl sulfoxide (DMSO), etc., making it a suitable interfacial layer material for BHJ PSCs. The structure of **FN-C60** was confirmed by MALDI-TOF mass spectrum and proton NMR spectrum. All peaks in the proton NMR spectrum of **FN-C60** obtained in deuterated DMSO became broader. This is probably due to the fact that **FN-C60** is an amphiphilic molecule; it will form aggregates rather than real solution in polar solvents. UV−vis absorption spectra of **FN-C60** in methanol and $PC_{60}BM$ and **FBr-C60** in THF solutions are shown in Figure 1. Similar to $PC_{60}BM$, **FBr-C60** and **FN-C60** showed two absorption peaks: a strong absorption peak in short wavelength region around at 327 nm and a weak absorption peak at about 430 nm. Obviously, the quaternization has no significnat influence on the optical properties of **FN-C60**.

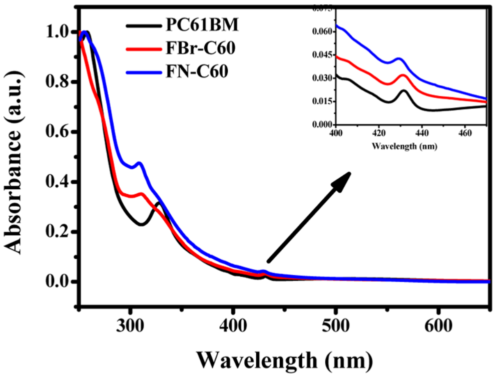

Figure 1. UV−vis absorption spectra of $PC_{61}BM$ and **FBr-C60** in THF and **FN-C60** in methanol.

Electrochemical Properties. Cyclic voltammetry was carried out to investigate the electrochemical properties of $PC_{61}BM$ and **FBr-C60** in $DCB:CH_3CN$ (1:4, v/v) and **FN-C60** in CH_3CN. Cyclic voltammograms of **FBr-C60** and $PC_{61}BM$ are shown in Figure 2a. Similar to $PC_{61}BM$, **FBr-C60** exhibited three well-defined reduction waves in the scanning range from 0 to −2.4 V. From the reduction curves, the reduction potentials were evaluated to be −0.99, −1.38, and −1.90 V for **FBr-C60** and −1.07, −1.47, and −1.97 V for $PC_{61}BM$ (Table 1). The reference electrode was calibrated by ferrocene/ferrocenium (Fc/Fc^+; 4.8 eV below vacuum level) to obtain accurate energy levels. The lowest unoccupied molecular orbital (LUMO) levels of **FBr-C60** and $PC_{61}BM$ were thus calculated to be −3.85 and −3.75 eV, respectively. Compared with **FBr-C60**, the quaternization process showed significant influence on the electrochemical properties of **FN-C60**. For **FN-C60**, it exhibited only one well-defined reduction wave in the scanning range, as shown in Figure 2b. From the reduction curve, the onset potential of this reduction wave was evaluated to be −1.14 V, correspoinding to the LUMO level of 3.57 eV.

Table 1. Half-Wave Reduction Potentials, Onset Reduction Potentials, and LUMO Energy Levels of $PC_{61}BM$ and FBr-C60 in $DCB:CH_3CN$ Solutions and FN-C60 in CH_3CN Solutions

fullerene derivatives	E_1(V)	E_2(V)	E_3(V)	E_{onset} (V)	LUMO (eV)
$PC_{61}BM$	−1.07	−1.47	−1.97	−0.96	−3.75
FBr-C60	−0.99	−1.38	−1.90	−0.86	−3.85
FN-C60	−1.36			−1.14	−3.57

Photovoltaic Properties. In order to evaluate the photovoltaic performance of **FN-C60** as the interfacial layer, two different device configurations, ITO/PEDOT:PSS/active layer/Al and ITO/PEDOT:PSS/active layer/**FN-C60**/Al, were utilized. And four different active layers, **P3**:$PC_{71}BM$, **HXS-1**:$PC_{71}BM$, **PDFCDTBT**:$PC_{71}BM$, and **PDPQTBT**:$PC_{71}BM$ were examined in this study.[51] The **P3**:$PC_{71}BM$ based solar cell with an Al cathode showed a V_{oc} of 0.79 V, an FF of 0.57, a J_{sc} of 7.73 mA/cm^2, and a PCE of 3.50%. When a 0.05% (w/v) solution of **FN-C60** in methanol was spin-coated onto the active layer, in comparison with the use of bare Al as the cathode, the V_{oc}, FF, and J_{sc} of **P3**:$PC_{71}BM$ based devices increased from 0.79 to 0.84 V, 0.57 to 0.65, and 7.73 to 8.56 mA/cm^2, respectively. As a result, the PCE value of devices was improved from 3.50% for bare Al cathode to 4.64% for **FN-C60**/Al cathode, which is a 33% increase of PCE.

Control devices were also fabricated to investigate the possible influence of methanol on the photovoltaic performance. Control experiments showed that the treatment of the active layer with methanol had a positive effect on device performance. The PCE was improved slightly from 3.50 to 3.79% (see the Supporting Information). It is worth noting that the FF values of methanol treated devices are markedly lower than that of the **FN-C60** treated devices. Therefore we can make a conclusion that the improvement of device performance is mainly due to the effect of the **FN-C60** interfacial layer.

To testify to the widespread application for **FN-C60** as the interfacial layer material, narrow band gap polymer **HXS-1**, was

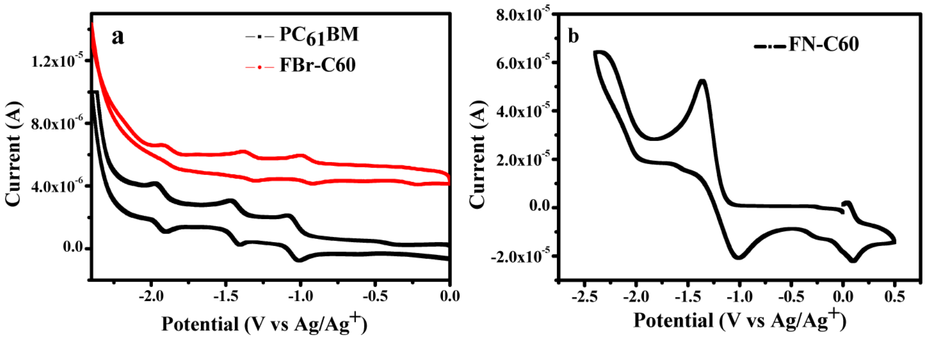

Figure 2. Electrochemical properties of $PC_{61}BM$ and **FBr-C60** in $DCB:CH_3CN$ (1:4, v/v) (a) and **FN-C60** in CH_3CN solution (b).

also investigated. The results are shown in Table 2. Using a bare Al cathode, a PCE of 4.27% with a V_{oc} of 0.82 V, an FF of 0.65, and a J_{sc} of 8.09 mA/cm^2 was achieved for **HXS-1**:PC$_{71}$BM based solar cells. When a thin layer of **FN-C60** was used as the interfacial layer between the active layer and the Al cathode, the PCE of **HXS-1**:PC$_{71}$BM based solar cells was dramatically increased to 5.25% with a V_{oc} of 0.86 V, an FF of 0.70, and a J_{sc} of 8.74 mA/cm^2. The typical current density–voltage (*J*–*V*) curves of photovoltaic cells with and without **FN-C60** as the interlayer are shown in Figure 3. External quantum efficiency (EQE) curves of **P3**:PC$_{71}$BM and **HXS-1**:PC$_{71}$BM based BHJ PSCs with and without the interfacial layer measured under illumination of monochromatic light are shown in Figure 3b. For both polymers, broad photocurrent responses from 300 to 700 nm can be observed. The EQE values of BHJ PSCs using the **FN-C60** interfacial layer are higher than that without the interfacial layer. All current density (J_{sc}) values calculated from the integration of the EQEs of the devices agree well with that obtained from the *J*–*V* measurements.

Table 2. Photovoltaic Parameters of the Devices Based on Bare Al Cathode, FN-C60/Al Cathode, and LiF/Al Cathode

active layer	interfacial layer	V_{oc} (V)	J_{sc} (mA/cm^2)	FF	Eff (%)	Rs (Ω/cm^2)
P3:PC$_{71}$BM	no	0.79	7.73	0.57	3.50	5.8
	FN-C60	0.84	8.56	0.65	4.64	4.5
	LiF	0.82	8.32	0.63	4.30	5.2
HXS-1:PC$_{71}$BM	no	0.82	8.09	0.65	4.27	3.1
	FN-C60	0.86	8.74	0.70	5.25	2.1
	LiF	0.82	8.58	0.67	4.69	3.3

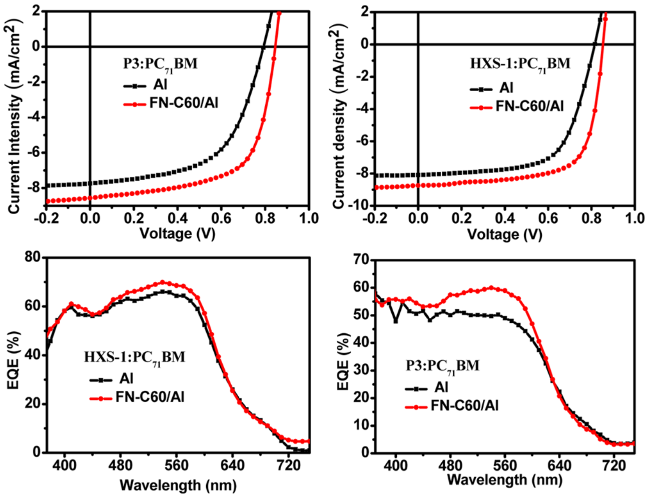

Figure 3. (a) *J*–*V* curves for the BHJ solar cells derived with the bare Al cathode and **FN-C60**/Al cathode from the blend of polymer:PC$_{71}$BM (1:3, by weight). (b) EQE curves for the BHJ solar cells derived with the bare Al cathode and **FN-C60**/Al cathode from the blend of polymer:PC$_{71}$BM (1:3, by weight).

In addition, the devices with an LiF/Al cathode were fabricated for the active layer of **P3**:PC$_{71}$BM and **HXS-1**:PC$_{71}$BM for a comparison. The photovoltaic parameters are shown in Table 2. The devices with LiF/Al cathode for **P3**:PC$_{71}$BM showed the maxium PCE of 4.30% with a V_{oc} of 0.82 V, an FF of 0.63, and a J_{sc} of 8.32 mA/cm^2, which is lower than the device with the **FN-C60**/Al cathode. Similarly, in the case of the devices with the LiF/Al cathode for **HXS-1**:PC$_{71}$BM, the maxium PCE of 4.69% was obtained with a V_{oc} of 0.82 V, an FF of 0.67, and a J_{sc} of 8.58 mA/cm^2. Obviously, the results are consistent with the devices for **P3** based PSCs. Therefore, the overall photovoltaic characteristics of PSCs with the **FN-C60**/Al cathode were comparable to and even better than those with LiF/Al cathode, indicating that alcohol soluble fullerene derivative **FN-C60** is promising as an interfacial layer material for PSCs.

In order to confirm that the use of **FN-C60** as the interfacial layer between the active layer and Al cathode can effectively reduce contact resistance of polymer solar cells, series resistance (Rs) values were determined from the inverse slope near V_{oc} in the *J*–*V* curves shown in Figure 3, and Rs values are also listed in Table 2. For both **P3** and **HXS-1** based solar cells, the Rs of devices using the **FN-C60**/Al cathode is smaller than that of devices using the bare Al cathode, indicating that the use of the **FN-C60** interfacial layer can improve the interface contact between the active layer and the Al electrode.[52,53] More polymer systems have been tried, and **FN-C60** also showed a positive effect on photovoltaic performance as shown in Table 3.

CONCLUSIONS

In conclusion, we have demonstrated that alcohol soluble fullerene derivative **FN-C60** can be used as an efficient interfacial layer between the active layer and Al cathode for low-cost and high-efficiency PSCs. The introduction of an **FN-C60** interfacial layer can increase the PCE of polymer solar cells for about 20–70%, which can be attributed to the improvement of interface contact and its *n*-type nature for better electron transportation and collection. In comparison with the Li/Al cathode, the better photovoltaic performance and the easy solution processability made **FN-C60** a promising interfacial layer material for the fabrication of low cost and high efficiency polymer solar cells. More detailed studies on this new highly efficient alcohol soluble interfacial material are currently underway.

Table 3. Photovoltaic Parameters of the Devices Based on the Bare Al Cathode, FN-C60/Al Cathode, and LiF/Al Cathode

active layer	interfacial layer	V_{oc} (V)	J_{sc} (mA/cm^2)	FF	Eff (%)
PDFCDTBT:PC$_{71}$BM[a] (1:1.8)	no	0.77	8.58	0.41	2.70
	FN-C60	0.94	8.65	0.57	4.64
	LiF	0.84	8.68	0.53	3.86
PDPQTBT:PC$_{71}$BM[b] (1:3)	no	0.77	4.3	0.46	1.52
	FN-C60	0.98	4.4	0.53	2.29
	LiF	0.83	4.4	0.48	1.75

[a] TCB/CN (10%). [b] DCB.

ASSOCIATED CONTENT

Supporting Information

Synthesis and characterizations of compound **2**, **FBr-C60**, and **FN-C60**; experimental details for the fabrication and measurements of polymer solar cells; ^{1}H NMR spectra and MALDI-TOF mass spectra of **FBr-C60** and **FN-C60**. This material is available free of charge via the Internet at http://pubs.acs.org.

AUTHOR INFORMATION

Corresponding Author

*E-mail addresses: licuihong@bnu.edu.cn (C.L.); zsbo@bnu.edu.cn (Z.B.).

Notes

The authors declare no competing financial interest.

ACKNOWLEDGMENTS

We express thanks for the financial support by the NSF of China (51003006, 91233205, and 21161160443), the 973 Programs (2011CB935702 and 2009CB623603), and the Fundamental Research Funds for the Central Universities.

REFERENCES

(1) Yu, G.; Heeger, A. J. *J. Appl. Phys.* **1995**, *78*, 4510−4515.

(2) Kim, J. Y.; Lee, K.; Coates, N. E.; Moses, D.; Nguyen, T. Q.; Dante, M.; Heeger, A. J. *Science* **2007**, *317*, 222−225.

(3) Hou, J. H.; Chen, H. Y.; Zhang, S. Q.; Li, G.; Yang, Y. *J. Am. Chem. Soc.* **2008**, *130*, 16144−16145.

(4) Chen, J. W.; Cao, Y. *Acc. Chem. Res.* **2009**, *42*, 1709−1718.

(5) Krebs, F. C. *Sol. Energ. Mat. Sol. C.* **2009**, *93*, 394−412.

(6) Brabec, C. J.; Gowrisanker, S.; Halls, J. J. M.; Laird, D.; Jia, S. J.; Williams, S. P. *Adv. Mater.* **2010**, *22*, 3839−3856.

(7) Zhan, X. W.; Zhu, D. B. *Polym. Chem.* **2010**, *1*, 409−419.

(8) Gendron, D.; Leclerc, M. *Energ. Environ. Sci.* **2011**, *4*, 1225−1237.

(9) He, Z. C.; Zhong, C. M.; Huang, X.; Wong, W. Y.; Wu, H. B.; Chen, L. W.; Su, S. J.; Cao, Y. *Adv. Mater.* **2011**, *23*, 4636−4643.

(10) Dou, L. T.; Gao, J.; Richard, E.; You, J. B.; Chen, C. C.; Cha, K. C.; He, Y. J.; Li, G.; Yang, Y. *J. Am. Chem. Soc.* **2012**, *134*, 10071−10079.

(11) Li, W. W.; Roelofs, W. S. C.; Wienk, M. M.; Janssen, R. A. J. *J. Am. Chem. Soc.* **2012**, *134*, 13787−13795.

(12) Small, C. E.; Chen, S.; Subbiah, J.; Amb, C. M.; Tsang, S. W.; Lai, T. H.; Reynolds, J. R.; So, F. *Nat. Photonics* **2012**, *6*, 115−120.

(13) Qin, R. P.; Li, W. W.; Li, C. H.; Du, C.; Veit, C.; Schleiermacher, H. F.; Andersson, M.; Bo, Z. S.; Liu, Z. P.; Inganas, O.; Wuerfel, U.; Zhang, F. L. *J. Am. Chem. Soc.* **2009**, *131*, 14612−14613.

(14) Li, W.; Qin, R.; Zhou, Y.; Andersson, M.; Li, F.; Zhang, C.; Li, B.; Liu, Z.; Bo, Z.; Zhang, F. *Polymer* **2010**, *51*, 3031−3038.

(15) Du, C.; Li, C. H.; Li, W. W.; Chen, X.; Bo, Z. S.; Veit, C.; Ma, Z. F.; Wuerfel, U.; Zhu, H. F.; Hu, W. P.; Zhang, F. L. *Macromolecules* **2011**, *44*, 7617−7624.

(16) He, Z. C.; Zhong, C. M.; Su, S. J.; Xu, M.; Wu, H. B.; Cao, Y. *Nat. Photonics* **2012**, *6*, 591−595.

(17) Heliatek GmbH, Dresden, Germany. http://www.heliatek.com (accessed June 28, 2013).

(18) Brabec, C. J.; Cravino, A.; Meissner, D.; Sariciftci, N. S.; Fromherz, T.; Rispens, M. T.; Sanchez, L.; Hummelen, J. C. *Adv. Funct. Mater.* **2001**, *11*, 374−380.

(19) Brabec, C. J.; Cravino, A.; Meissner, D.; Sariciftci, N. S.; Rispens, M. T.; Sanchez, L.; Hummelen, J. C.; Fromherz, T. *Thin Solid Films* **2002**, *403*, 368−372.

(20) Mihailetchi, V. D.; Koster, L. J. A.; Blom, P. W. M. *Appl. Phys. Lett.* **2004**, *85*, 970−972.

(21) Hau, S. K.; O'Malley, K. M.; Cheng, Y. J.; Yip, H. L.; Ma, H.; Jen, A. K. Y. *Ieee. J. Sel. Top. Quant.* **2010**, *16*, 1665−1675.

(22) Mihailetchi, V. D.; Blom, P. W. M.; Hummelen, J. C.; Rispens, M. T. *J. Appl. Phys.* **2003**, *94*, 6849−6854.

(23) Ratcliff, E. L.; Zacher, B.; Armstrong, N. R. *J. Phys. Chem. Lett.* **2011**, *2*, 1337−1350.

(24) Walzer, K.; Maennig, B.; Pfeiffer, M.; Leo, K. *Chem. Rev.* **2007**, *107*, 1233−1271.

(25) Clarke, T. M.; Durrant, J. R. *Chem. Rev.* **2010**, *110*, 6736−6767.

(26) Waldauf, C.; Morana, M.; Denk, P.; Schilinsky, P.; Coakley, K.; Choulis, S. A.; Brabec, C. J. *Appl. Phys. Lett.* **2006**, *89*, 233517.

(27) White, M. S.; Olson, D. C.; Shaheen, S. E.; Kopidakis, N.; Ginley, D. S. *Appl. Phys. Lett.* **2006**, *89*, 143517.

(28) Brabec, C. J.; Shaheen, S. E.; Winder, C.; Sariciftci, N. S.; Denk, P. *Appl. Phys. Lett.* **2002**, *80*, 1288−1290.

(29) Hau, S. K.; Yip, H. L.; Chen, K. S.; Zou, J. Y.; Jen, A. K. Y. *Appl. Phys. Lett.* **2010**, *97*, 253307.

(30) Yip, H. L.; Hau, S. K.; Baek, N. S.; Ma, H.; Jen, A. K. Y. *Adv. Mater.* **2008**, *20*, 2376−2382.

(31) Tao, C.; Ruan, S. P.; Zhang, X. D.; Xie, G. H.; Shen, L.; Kong, X. Z.; Dong, W.; Liu, C. X.; Chen, W. Y. *Appl. Phys. Lett.* **2008**, *93*, 193307.

(32) Goh, C.; Scully, S. R.; McGehee, M. D. *J. Appl. Phys.* **2007**, *101*, 114503.

(33) Kim, J. Y.; Kim, S. H.; Lee, H. H.; Lee, K.; Ma, W. L.; Gong, X.; Heeger, A. J. *Adv. Mater.* **2006**, *18*, 572−576.

(34) Park, S. H.; Roy, A.; Beaupre, S.; Cho, S.; Coates, N.; Moon, J. S.; Moses, D.; Leclerc, M.; Lee, K.; Heeger, A. J. *Nat. Photonics.* **2009**, *3*, 297−302.

(35) Sun, Y. M.; Seo, J. H.; Takacs, C. J.; Seifter, J.; Heeger, A. J. *Adv. Mater.* **2011**, *23*, 1679−1683.

(36) You, J. B.; Chen, C. C.; Dou, L. T.; Murase, S.; Duan, H. S.; Hawks, S. A.; Xu, T.; Son, H. J.; Yu, L. P.; Li, G.; Yang, Y. *Adv. Mater.* **2012**, *24*, 5267−5272.

(37) Huang, F.; Wu, H. B.; Cao, Y. *Chem. Soc. Rev.* **2010**, *39*, 2500−2521.

(38) He, Z. C.; Zhang, C.; Xu, X. F.; Zhang, L. J.; Huang, L.; Chen, J. W.; Wu, H. B.; Cao, Y. *Adv. Mater.* **2011**, *23*, 3086−3089.

(39) Seo, J. H.; Gutacker, A.; Sun, Y. M.; Wu, H. B.; Huang, F.; Cao, Y.; Scherf, U.; Heeger, A. J.; Bazan, G. C. *J. Am. Chem. Soc.* **2011**, *133*, 8416−8419.

(40) Tang, Z.; Andersson, L. M.; George, Z.; Vandewal, K.; Tvingstedt, K.; Heriksson, P.; Kroon, R.; Andersson, M. R.; Inganas, O. *Adv. Mater.* **2012**, *24*, 554−558.

(41) Duan, C. H.; Zhong, C. M.; Liu, C. C.; Huang, F.; Cao, Y. *Chem. Mater.* **2012**, *24*, 1682−1689.

(42) Lee, R. H.; Syu, J. Y.; Huang, J. L. *Polym. Adv. Technol.* **2011**, *22*, 2110−2122.

(43) Schulze, K.; Uhrich, C.; Schuppel, R.; Leo, K.; Pfeiffer, M.; Brier, E.; Reinold, E.; Bauerle, P. *Adv. Mater.* **2006**, *18*, 2872−2875.

(44) Cheng, Y. J.; Cao, F. Y.; Lin, W. C.; Chen, C. H.; Hsieh, C. H. *Chem. Mater.* **2011**, *23*, 1512−1518.

(45) Hsieh, C. H.; Cheng, Y. J.; Li, P. J.; Chen, C. H.; Dubosc, M.; Liang, R. M.; Hsu, C. S. *J. Am. Chem. Soc.* **2010**, *132*, 4887−4893.

(46) O'Malley, K. M.; Li, C. Z.; Yip, H. L.; Jen, A. K. Y. *Adv. Energy. Mater.* **2012**, *2*, 82−86.

(47) Li, C. Z.; Chueh, C. C.; Yip, H. L.; O'Malley, K. M.; Chen, W. C.; Jen, A. K. Y. *J. Mater. Chem.* **2012**, *22*, 8574−8578.

(48) Wang, S.; Liu, B.; Gaylord, B. S.; Bazan, G. C. *Adv. Funct. Mater.* **2003**, *13*, 463−467.

(49) Zhu, B.; Han, Y.; Sun, M. H.; Bo, Z. S. *Macromolecules* **2007**, *40*, 4494−4500.

(50) Wei, X. W.; Avent, A. G.; Boltalina, O. V.; Street, J. M.; Taylor, R. *J. Chem. Soc. Perkin Trans. 2* **2002**, 47−52.

(51) Jin, E. Q.; Du, C.; Wang, M.; Li, W. W.; Li, C. H.; Wei, H. D.; Bo, Z. S. *Macromolecules* **2012**, *45*, 7843−7854.

(52) Potscavage, W. J.; Sharma, A.; Kippelen, B. *Acc. Chem. Res.* **2009**, *42*, 1758−1767.

(53) Blom, P. W. M.; Mihailetchi, V. D.; Koster, L. J. A.; Markov, D. E. *Adv. Mater.* **2007**, *19*, 1551−1566.